

# Study of Curing of Layered Silicate/Trifunctional Epoxy Nanocomposites by Means of FTIR Spectroscopy

P. Pagès,<sup>1</sup> T. Lacorte,<sup>1</sup> M. Lipinska,<sup>2</sup> F. Carrasco<sup>3</sup>

<sup>1</sup>Department of Material Science, Universitat Politècnica de Catalunya, Terrassa 08222, Spain

<sup>2</sup>Institute of Polymer and Dye Technology, Technical University of Lodz, Lodz 90-924, Poland

<sup>3</sup>Department of Chemical Engineering, Universitat de Girona, Girona 17071, Spain

Received 24 March 2007; accepted 12 November 2007

DOI 10.1002/app.27853

Published online 4 February 2008 in Wiley InterScience (www.interscience.wiley.com).

**ABSTRACT:** A study was conducted on the curing process of a nanocomposite consisting of a trifunctional epoxy resin, a hardener containing reactive primary amine groups, and montmorillonite (MMT) nanoparticles, previously treated with octadecyl ammonium. Three levels of MMT content were used: 2, 5, and 10%. The curing was carried out following the cycle: 4 h at 100°C, 2 h at 150°C, and 2 h at 200°C. Isothermal trials were also considered at three levels (120, 150, and 200°C) to conduct a kinetic study. The curing conversion was determined by FTIR spectroscopy by selecting the suitable bands for epoxide

and primary amine functional groups. The study demonstrated that the MMT nanoparticles accelerate the curing process, especially at the initial stages of the thermal cycle, being this influence quasi negligible at the end of the cycle. Curing conversions were also evaluated by differential scanning calorimetry and compared to those obtained by FTIR spectroscopy. © 2008 Wiley Periodicals, Inc. *J Appl Polym Sci* 108: 2107–2115, 2008

**Key words:** nanocomposites; resins; curing of polymers; FTIR; kinetics

## INTRODUCTION

As a result of advances in nanotechnology, new materials called polymer nanocomposites are receiving increasing attention. These materials consist of a polymer matrix (epoxy resin, starch, polyurethane, polylactic acid, poly(ethylene terephthalate), silylated poly(urethane-urea), poly(vinyl alcohol), polyetherimide, polypropylene, and polyethylene), and nanoparticles (carbon nanotubes, fumed silica, microcrystalline cellulose, and various types of clays). These materials are of great interest from an industrial and scientific perspective because they show much better behavior and characteristics in comparison with conventional composites.<sup>1–14</sup>

In the 1980s, Dow Chemicals introduced a new generation of multifunctional epoxy resins (with a level of functionality of 3 to 5) that had a great impact on the market because their properties were better than those of earlier conventional (i.e., bifunctional) epoxy resins.<sup>15</sup> For the same level of curing, multifunctional resins have better crosslink densities and glass transition temperatures, providing a con-

siderable increase in their thermal, dynamic, mechanical, and adhesive properties in comparison with their bifunctional predecessors.<sup>16,17</sup>

Of these multifunctional epoxy resins, a trifunctional resin derived from *p*-aminophenol produced by Vantico is widely used in adhesive and structural applications. This resin is notable for its low viscosity, the fact that it can be cured at reasonable temperatures and its excellent properties at high temperatures. The resin is of the same type as that used as the matrix of the nanocomposites prepared for this study and we had previously studied its curing process using FTIR spectroscopy and differential scanning calorimetry.<sup>15</sup> A product with primary amine-based reactive groups was used as a hardener. The same resin/hardener system was used in this study, with the additional dispersion of certain proportions (2, 5, and 10%, by weight) of layered silicate nanoparticles to obtain the nanocomposites. The material curing was then monitored by using FTIR spectroscopy. Epoxide and primary amine bands were selected to determine the curing conversion. These results were also compared to those obtained by differential scanning calorimetry (DSC).

The dispersion of the nanoparticles, practically at atomic level, and their surface treatment using alkylammonium cations, which compete with the hardener in the resin-curing process and act as an accelerant, are factors that will presumably give rise to notable differences in the curing of the resin/hardener system used as the nanocomposite matrix, compared

Correspondence to: F. Carrasco (felix.carrasco@udg.edu).

Contract grant sponsor: Ministry of Education and Science of the Spanish Government; contract grant numbers: MAT2003-04, 853.

to the previously studied curing mechanism of the same system without the nanoparticles.<sup>15,18</sup>

## EXPERIMENTAL METHODS

### Materials

The matrix was a trifunctional epoxy resin (TGAP), marketed as Araldite MY510 from Vantico, with a viscosity at 25°C of 0.55–0.85 Pa s, density of 1205–1225 kg/m<sup>3</sup>, and a maximum moisture content of 0.20%. The hardener used was 4,4' diaminodiphenylsulfone, marketed as HT-976-1, from Vantico. The nanoparticles consisted of montmorillonite (MMT) layered silicate, treated with the surfactant octadecyl ammonium, with particle length ranging between 100 and 150 nm and thickness of ~1 nm and marketed as Nanomer I.30E from Nanocor (Arlington Heights, Illinois).

### Preparation of the nanocomposites

Organic solvents such as acetone, which are often used to prepare this type of material, were avoided because of their harmful effect on the environment. Some references in the literature<sup>19,20</sup> were taken into consideration and several improvements stemming from our experience in preparing nanocomposites were adopted to achieve a correct dispersion of the nanoparticles in the matrix. The mixture of resin and MMT was prepared in the appropriate quantities to obtain nanocomposites with the desired proportion of nanoparticles (2, 5, and 10%, by mass) and mixed by hand for 2 min. The mixture was then placed in an ultrasound bath for 1 h to ensure correct dispersion. The dispersion of MMT particles in the matrix was monitored using wide-angle X-ray scattering techniques and optical microscopy with polarized light. Both tests showed satisfactory particle dispersion with no formation of any aggregates of note. The mixture was then heated to 80°C. This temperature was maintained while the hardener was slowly added. The mixture was then stirred for 20 min. The ratio of resin to hardener, by mass, was 100/52, which corresponds to a slight excess of primary amine groups with respect to the epoxide groups present in the resin. To prepare the nanocomposite correctly, it was essential to remove the entrapped air by placing it in a vacuum oven until all bubbles were seen to be gone from the mixture. This air removal is particularly important in terms of the mechanical properties of the material.

### Materials curing

Small amounts of the above mixtures (200 mg) were deposited on NaCl crystal, placed in an oven at 25°C, and heated to 100°C at a rate of 2.5°C/min.

This temperature was maintained for 4 h. The temperature was then increased to 150°C for 2 h and finally to 200°C for 2 h. This is the thermal cycle employed in our study. Such a cycle was modified by the authors (with respect to that recommended by the supplier for the resin/hardener) to take into account the higher reactivity of our materials when nanoparticles treated with octadecyl ammonium were incorporated. On the other hand, isothermal trials at three levels (120, 150, and 200°C) were carried out to study the influence of temperature in the curing process as well as to conduct a kinetic study.

### Monitoring of curing by means of FTIR spectroscopy

The spectra of the mixtures on the NaCl substrate were recorded before they were placed in the oven for heat treatment. Once they were in the oven, their spectra were recorded every hour until the treatment had completely finished (for experiments conducted following the thermal cycle) and every 10 min for isothermal experiments. It has to be noted that a different sample was used for each curing time to avoid breaks during the heat treatment. A Nicolet 510M spectrophotometer was used for this purpose.

### Monitoring of curing by means of DSC

DSC measurements were performed using a Mettler Toledo DSC821 equipped with an intracooler and robot sample placer. All DSC experiments were conducted with a flow of dry nitrogen at 50 mL/min. Samples of about 10 mg were sealed in standard aluminum pans with a hole in the lid. To study the isothermal cure reaction, the samples were placed exactly at the temperature of the measurements, each sample was cured in the DSC for the required time (10, 20, 30, 40, 50, 60, 120, and 180 min) at the selected temperature, and then cooled to 25°C at –10 K/min. The degree of cure was determined from the second scan at 10 K/min from 25 to 300°C, from which the residual heat of cure was found. The degree of cure determined by DSC was calculated according to the equation:  $\alpha = 1 - \Delta H_{\text{res}}/\Delta H_{\text{tot}}$  where  $\Delta H_{\text{res}}$  is the residual heat of cure after the partial isothermal cure and  $\Delta H_{\text{tot}}$  is the total heat of cure. To investigate the glass transition of the cured samples, the samples were heated at 10 K/min from 25 to 300°C. The glass transition temperatures were evaluated as the mid-point temperatures determined using the Mettler Toledo STAR software.

## RESULTS AND DISCUSSION

Figures 1 and 2 show the spectra (4000–3000 and 1000–750 cm<sup>-1</sup>) for the nanocomposite containing

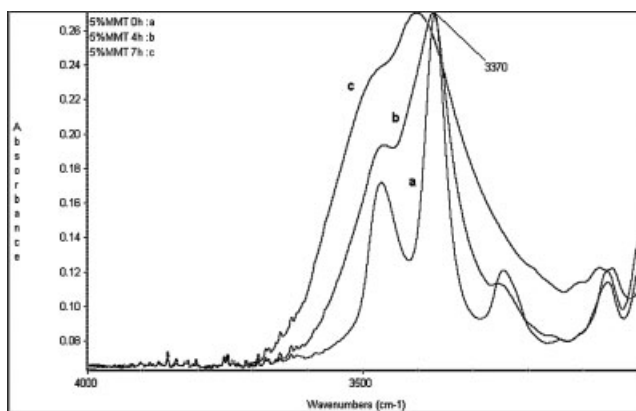


**Figure 1** FTIR spectra in the 4000–3000  $\text{cm}^{-1}$  region (primary amine groups) for the nanocomposite with 5% of montmorillonite (MMT) at various stages of curing. (a) 0 h; (b) 4 h; (c) 7 h.

5% of MMT at various stages in the curing cycle. The curing process was studied by evaluating the decrease of the specific band of the primary amine groups (Fig. 1) and that of the epoxide groups (Fig. 2). The band that appears at 3370  $\text{cm}^{-1}$  (Fig. 1) was used for the primary amine groups and that at 906  $\text{cm}^{-1}$  (Fig. 2) for the epoxide groups. These are the most suitable bands, even if there was a partial overlapping, as it will be discussed later. The decrease in the absorbance of these bands was used to follow the progress of cure reactions. Thus, for each of the nanocomposites obtained, the curing progress was followed by calculating the curing conversion,  $\alpha = 1 - A^*(t)/A^*(0)$ , where  $A^*(t)$  and  $A^*(0)$  are the reduced absorbance at time  $t$  and at starting time, respectively, corresponding to the aforementioned vibration bands. The band of the benzene ring, which appears at 1513  $\text{cm}^{-1}$ , was chosen as an invariant reference band and was used to calculate the reduced absorbance for both epoxide and primary amine groups.

Even if the height of the band at 3370  $\text{cm}^{-1}$  (primary amine groups, as seen in Fig. 1) seems not to vary as a function of time, it is only a visual effect, because this parameter experienced a significant change when calculating it by using the “baseline method” (i.e., the final absorbance was determined by calculating the difference between the registered absorbance and the baseline). Therefore, the absorbance was calculated as the height between the maximum absorbance of the selected peak and the baseline at the same wavenumber. The baseline can be plotted over the spectral region of interest (in our study for the region covering the three peaks, within the wavenumber range 3700–3100  $\text{cm}^{-1}$ ) or over the selected peak (in this case, the baseline was obtained by plotting the tangent line between the minimum

absorbances of the selected peak). Obviously, both baseline procedures led to different heights, but the conversion values were very similar. This finding confirmed that the partial overlapping (at the right and the left of the selected band) did not affect the peak height. Moreover, we have deconvoluted the spectral region covering the three peaks within the region 3700–3100  $\text{cm}^{-1}$ . The results obtained indicated that the deconvolution of the three peaks did not modify the value of the conversion calculated by using the area of the peak at 3370  $\text{cm}^{-1}$ . This again proved that the partial overlapping of the selected peak had no influence on conversion calculations. It has to be noted that similar results were obtained for bands at 906  $\text{cm}^{-1}$  (epoxide groups, as seen in Fig. 2). Finally, the correctness of the method applied to calculate FTIR conversion was corroborated by means of DSC and it will be discussed later.

Figure 3 shows the variation of the epoxide conversion as a function of curing time for the curing schedule employed in our study. In the initial stages of curing, it was observed that a greater proportion of MMT in the nanocomposite led to higher epoxide conversions. After 2 h at 100°C, the epoxide conversions were 11, 25, and 44% for 2, 5, and 10% MMT content, respectively, and the mean curing rates were 5.5, 12.5, and 22%/h. Therefore, an increase in the nanoparticles content had a beneficial effect on the reaction rate (i.e., during this period, the mean reaction rate at 200°C was 4.0 times higher than at 100°C). It is also of note that the higher proportions of MMT (5 and 10%) caused significant increase in epoxide conversion after only 1 h of heat treatment at 100°C (14 and 31%, respectively). At the lower level of MMT (2%), the curing was not detected during this first hour of curing. These findings demonstrate and confirm that the surface modifier (octa-

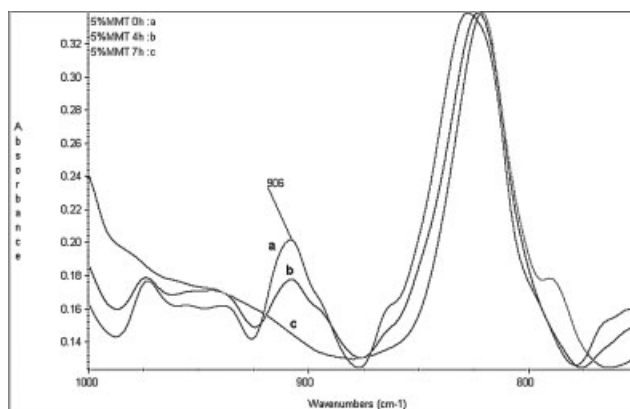


**Figure 2** FTIR spectra in the 1000–750  $\text{cm}^{-1}$  region (epoxide groups) for the nanocomposite with 5% of montmorillonite (MMT) at various stages of curing. (a) 0 h; (b) 4 h; (c) 7 h.

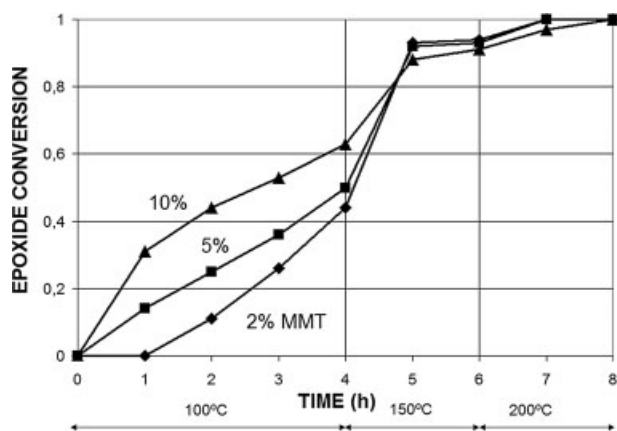


**Figure 3** Variation of the epoxide conversion (at  $906\text{ cm}^{-1}$ ) as a function of curing time for the nanocomposites containing 2, 5, and 10% of montmorillonite (MMT), for the thermal cycle treatments.

decyl ammonium) of the MMT accelerates the curing process, as previously reported by Triantafillidis et al.<sup>21</sup> They demonstrated that acidic onium ions (i.e., acidic cations) of diamines catalyze the intragallery epoxide polymerization process. The greater reactivity of the ammonium surface modifier explains why a greater proportion of MMT in the nanocomposite increases the epoxide conversion in the initial curing stages. On the contrary, in the final curing stages, the accelerant effect is cancelled out and inverted because of the barrier effect caused by the exfoliated MMT nanoparticles inside the matrix. Once most of the covalent crosslinking between molecular chains has taken place, a greater presence of MMT would contribute to blocking completion of the curing process of the matrix, which now has a higher crosslink density, since the exfoliated nanoparticles between the chains act as physical barriers, severely restricting the mobility of the resin polymer chains. The foregoing is in accordance with the values of conversion obtained for the nanocomposites studied. MMT contents of 2, 5, and 10% led to epoxide conversions of 93, 92, and 88%, respectively, for 5 h treatments (4 h at  $100^\circ\text{C}$  and 1 h at  $150^\circ\text{C}$ ). Total curing was reached after 7 h of heat treatment for the nanocomposites with 2 and 5% of MMT. The nanocomposite with 10% of MMT did not reach total curing until after 8 h of treatment. Total curing (as monitored by FTIR spectroscopy) was also confirmed by performing DSC tests under the conditions set out in previous experiments.<sup>15</sup> The DSC tests showed that the glass transition temperature of all the nanocomposites studied was located within the range  $230\text{--}240^\circ\text{C}$  (depending on both curing temperature and conversion). The arguments presented in this study agree with the results previously obtained by the authors<sup>15</sup> when they studied the curing of the same resin/hardener material without

MMT nanoparticles. The absence of the octadecyl ammonium accelerant led to slower curing at all stages and total curing required longer heat treatment.

It has to be noted that the curing progress can also be studied by evaluating the decrease observed in the bands of the spectra corresponding to the primary amine groups. Figure 4 shows the evolution of the amine conversion for the different proportions of MMT used. The results obtained showed similar trends to those reported for the epoxide conversion. In the initial stages of curing, it was observed that a greater proportion of MMT in the nanocomposite led to a higher amine conversion. After 2 h at  $100^\circ\text{C}$ , the amine conversions were 17, 27, and 50% for 2, 5, and 10% of MMT, respectively, and the mean curing rates were 9.5, 13.5, and 25%/h. Therefore, an increase in the nanoparticles content had a beneficial effect on the reaction rate (i.e., during this period, the mean reaction rate at  $200^\circ\text{C}$  was 2.6 times higher than at  $100^\circ\text{C}$ ). It is also of note that the higher proportions of MMT (5 and 10%) caused significant increase in amine conversion after only 1 h of heat treatment at  $100^\circ\text{C}$  (13 and 35%, respectively). At the lower level of MMT (2%), the curing was not detected during this first hour of curing, as previously reported for the epoxide conversion.

Figure 5 shows the comparison between epoxide and amine conversions. The excellent correlation between two different functional groups clearly indicates that partial overlapping (for epoxide bands as well as for amine bands) has no influence on conversion calculations. The epoxide conversion was slightly lower than the amine conversion, within the conversion range of 0–70%. Lower epoxide conversion (than that of primary amine) was also observed by Varley et al. when studying the reaction mechanism of different epoxy resins (bi, tri, and tetrafunc-

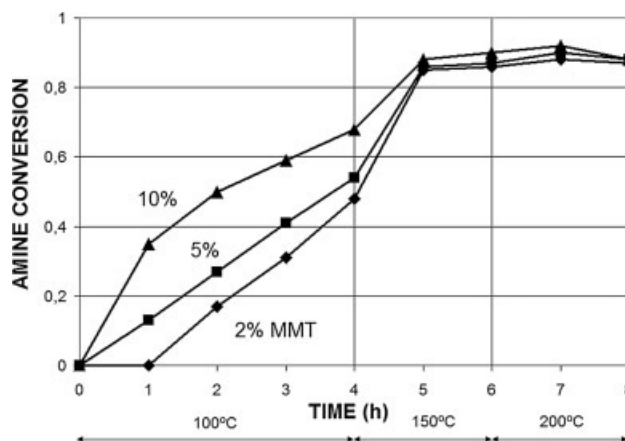


**Figure 4** Variation of the primary amine conversion (at  $3370\text{ cm}^{-1}$ ) as a function of curing time for the nanocomposites containing 2, 5, and 10% of montmorillonite (MMT), for the thermal cycle treatments.

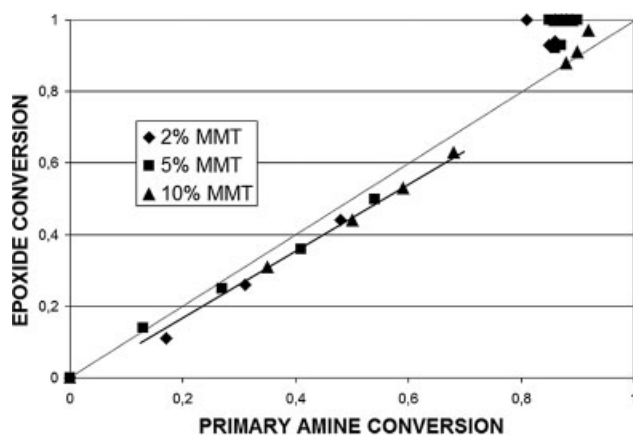


**Figure 5** Comparison of epoxide conversion (at  $906\text{ cm}^{-1}$ ) and primary amine conversion (at  $3370\text{ cm}^{-1}$ ) at the different stages of the thermal cycle used, for the nanocomposites containing 2, 5, and 10% of montmorillonite (MMT).

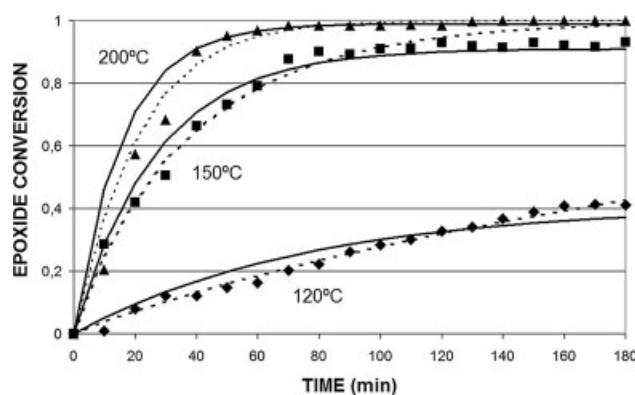
tional resins).<sup>22</sup> In the present work it was found an excellent correlation between both conversions:  $\alpha_{\text{epoxide}} = -0.015 + 0.931 \alpha_{\text{amine}}$  ( $r^2 = 0.988$ ). It means that the epoxide conversion was 93% of the amine conversion within the mentioned conversion range, and it was independent of the MMT content used. Even though the epoxide groups react with the primary amines from the beginning of the curing process, other reactions (i.e., not addition reactions) must exist that are responsible for the consumption of primary amine groups. At higher conversions (>80%), there was an inversion of this behavior: the epoxide conversion becomes higher than the amine conversion. It means that, at the end of the nanocomposite curing, the epoxide groups were totally consumed whereas the amine conversion was about 87–92%. In this conversion range, etherification reactions (i.e., homopolymerization) can explain the additional consumption of epoxide groups. Moreover, it must be taken into consideration that the hardener is present in a slight excess. When DSC tests were performed on the totally cured nanocomposites, the excess of hardener was confirmed with an endothermic peak at its melting temperature (i.e.,  $180^\circ\text{C}$ ).

Figure 6 shows the variation of epoxide conversion as a function of time for the three isothermal trials studied (at 120, 150, and  $200^\circ\text{C}$ ) by using materials with 5% of MMT nanoparticles. The curves were determined by using the kinetic data obtained by linear regression of two kinetic models: first-order kinetics (solid line) and Avrami theory (dotted line) and will be discussed later. There was a clear effect of temperature on nanocomposite curing. An asymptotic conversion value was reached, depending on the curing temperature: 41% at  $120^\circ\text{C}$ , 93% at  $150^\circ\text{C}$ , and 100% at  $200^\circ\text{C}$ . This finding indicates that there is a maximum conversion at each curing tempera-

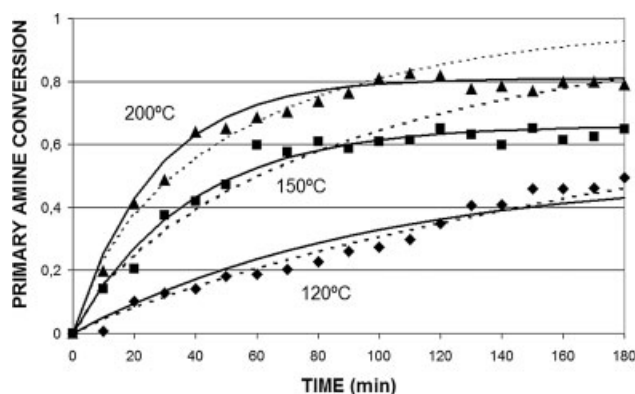
ture. Asymptotic values of conversion were also reported by Carrasco et al.<sup>15</sup> when curing the same epoxy resin without the presence of nanoparticles. Only at the highest temperature (i.e.,  $200^\circ\text{C}$ ) it was possible to attain the total nanocomposite curing. Therefore, there is a barrier effect at lower temperatures, not allowing the progression of curing reactions. On the other hand, during the initial stages of curing, the temperature had a very significant influence: During the first 20 min, the mean reaction rate was 0.4, 2.1, and 2.9%/min when the curing temperature was 120, 150, and  $200^\circ\text{C}$ , respectively. Therefore, the mean reaction rate during this period of time was 7.3 times higher at  $200^\circ\text{C}$  than at  $120^\circ\text{C}$ . After 1 h of isothermal treatment, the curing was quasi total at  $200^\circ\text{C}$  (97%), whereas the conversion was 79% at  $150^\circ\text{C}$  and 16% at  $120^\circ\text{C}$ . The maximum value of conversion was reached at 160 min (at  $120^\circ\text{C}$ ), 80 min (at  $150^\circ\text{C}$ ), and 60 min (at  $200^\circ\text{C}$ ).

Figure 7 shows the variation of primary amine conversion as a function of time for the three isothermal trials studied (at 120, 150, and  $200^\circ\text{C}$ ) by using materials with 5% of MMT nanoparticles. As previously indicated, the curves were determined by using the kinetic data obtained by linear regression of two kinetic models: first-order kinetics (solid line) and Avrami theory (dotted line). Again, an asymptotic conversion value was reached, depending on the curing temperature: 50% at  $120^\circ\text{C}$ , 66% at  $150^\circ\text{C}$ , and 83% at  $200^\circ\text{C}$ . These values are different from those found for epoxide groups. The trends of conversion of primary amine groups are quite similar to those previously reported for epoxide groups. Primary amine conversions never reached 100% because the epoxide groups are the limiting reactant.

The reaction mechanism and kinetics of the curing process for an epoxy resin as well as the presence of



**Figure 6** Variation of the epoxide conversion (at  $906\text{ cm}^{-1}$ ) as a function of curing time for the nanocomposites containing 5% of montmorillonite (MMT), for the isothermal curing at three temperature levels (120, 150, and  $200^\circ\text{C}$ ). Solid line: First-order kinetics; dotted line: Avrami equation.



**Figure 7** Variation of the primary amine conversion (at  $3370\text{ cm}^{-1}$ ) as a function of curing time for the nanocomposites containing 5% of montmorillonite (MMT), for the isothermal curing at three temperature levels (120, 150, and  $200^\circ\text{C}$ ). Solid line: First-order kinetics; dotted line: Avrami equation.

nanoparticles determine the morphology of the three-dimensional network, thus defining its physical and mechanical properties. It has been reported that the most important mechanical property of nanocomposites is their modulus of elasticity (related to the material rigidity) and the most significant physical property is their impermeability to gases, liquids, and radiations (due to the high aspect ratio of the nanoparticles and to the restricted mobility of the polymer chains which are near to the nanoparticles). There are two types of kinetic models: mechanistic and phenomenological. The mechanistic models are extremely complex because they imply identifying the elemental reactions and determining which of them is the rate-controlling step. Because of this, researchers have opted for the phenomenological models to study the curing process of thermoset materials. These models are very useful because they allow the overall rate of the process to be quantified, a variable which is fundamental to design the curing process reactor. The kinetic models most widely used are the  $n$ -order, autocatalytic, and diffusion controlled. The  $n$ -order kinetic model is frequently employed for all type of reactions because of its simplicity. Our experimental data presented poor adjustment when using the autocatalytic kinetic model, especially at the initial and final stages of the curing process, whereas there was an excellent correlation when the  $n$ -order kinetic model was employed.

The reaction rate was evaluated by the following expression:

$$\frac{d\alpha}{dt} = k(\alpha_m - \alpha)^n \quad (1)$$

This equation was modified by changing 1 (present in traditional equations) by the asymptotic con-

version reached at each temperature:  $\alpha_m = 0.41, 0.93,$  and 1 for 120, 150, and  $200^\circ\text{C}$ , respectively, for epoxide groups and 0.50, 0.66, and 0.83 for primary amine groups.

The integration of the eq. (1) leads to the following kinetic expressions for reaction orders 1 and 2.

$$\ln\left(1 - \frac{\alpha}{\alpha_m}\right) = -kt \quad n=1 \quad (2)$$

$$\frac{\alpha}{\alpha_m(\alpha_m - \alpha)} = kt \quad n=2 \quad (3)$$

By taking into consideration the previous equations, the half-life of the curing process can be evaluated as follows:

$$t_{1/2} = -\frac{1}{k} \ln\left(1 - \frac{1}{2\alpha_m}\right) \quad n=1 \quad (4)$$

$$t_{1/2} = -\frac{1}{k\alpha_m(2\alpha_m - 1)} \quad n=2 \quad (5)$$

The regression coefficients clearly indicate that the best fitting was obtained by using first-order kinetics. Table I shows the kinetic parameters (kinetic constant and activation energy) for the first-order disappearance of epoxide groups and primary amine groups (for the entire conversion range). The kinetic constants for the disappearance of epoxide groups were  $2.20 \times 10^{-4}, 6.28 \times 10^{-4},$  and  $10.5 \times 10^{-4}\text{ s}^{-1}$  when curing at 120, 150, and  $200^\circ\text{C}$ , respectively. Therefore, the reaction rate at  $150^\circ\text{C}$  was three times higher than that at  $120^\circ\text{C}$  and it was five times higher at  $200^\circ\text{C}$  than that at  $120^\circ\text{C}$ . By using the Arrhenius equation for the dependence of the kinetic constant on the temperature, the apparent activation energy was 29.5 kJ/mol. This value is lower than that reported for epoxy resins without nanoparticles (88.6 and 33.9 kJ/mol for the nonautocatalytic and autocatalytic reactions, respectively),<sup>15</sup> thus indicating the accelerant effect of the MMT nanoparticles in the curing process of epoxy resins.

**TABLE I**  
Kinetic Constant and Activation Energy Values Obtained by Linear Regression (According to First-Order Kinetics) for the Curing Process of the Nanocomposites

$T$ ( $^\circ\text{C}$ )	Epoxide groups		Primary amine groups	
	$k$ ( $\text{s}^{-1}$ ) ( $\alpha_m$ )	$r^2$	$k$ ( $\text{s}^{-1}$ ) ( $\alpha_m$ )	$r^2$
120	$2.20 \times 10^{-4}$ (0.41)	0.964	$1.72 \times 10^{-4}$ (0.50)	0.915
150	$6.28 \times 10^{-4}$ (0.93)	0.970	$4.44 \times 10^{-4}$ (0.66)	0.882
200	$10.5 \times 10^{-4}$ (1.00)	0.979	$6.29 \times 10^{-4}$ (0.83)	0.880
	$E_a = 29.5\text{ kJ/mol}$		$E_a = 24.2\text{ kJ/mol}$	

The half-life for the disappearance of epoxide groups was calculated to be 20 and 11 min at 150 and 200°C, respectively. On the other hand, the kinetic constants for the disappearance of primary amine groups were  $1.72 \times 10^{-4}$ ,  $4.44 \times 10^{-4}$ , and  $6.29 \times 10^{-4} \text{ s}^{-1}$  when curing at 120, 150, and 200°C, respectively. In this case, the apparent activation energy was 24.2 kJ/mol. Therefore, the activation barrier for primary amine groups is quite similar to that obtained for epoxide groups, thus confirming that the main reaction for the curing process was the polymerization between epoxide and primary amine groups.

The Avrami theory is widely accepted for describing the isothermal crystallization process and it is also used to describe the curing process, because the formation of microgels during the curing of thermoset materials can be compared to the spherulitic growth in crystallization. In other words, the number of microgels and their average diameter increase during the curing process, so the situation resembles that of polymer crystallization.<sup>23</sup> The Avrami equation, in its linear form, is the following:

$$\ln(1 - \alpha) = -kt^n \quad (6)$$

Therefore, the half-life can be calculated as follows:

$$t_{1/2} = \left( \frac{\ln 2}{k} \right)^{1/n} \quad (7)$$

Table II shows the kinetic parameters (kinetic constant and activation energy) for the disappearance of epoxide groups and primary amine groups according to Avrami equation. The kinetic constants for the disappearance of epoxide groups were  $1.25 \times 10^{-4}$ ,  $7.29 \times 10^{-4}$ , and  $9.42 \times 10^{-4} \text{ s}^{-1/n}$  when curing at 120, 150, and 200°C, respectively. The exponent  $n$  slightly varies with curing temperature, but takes a value near to 1. By using the Arrhenius equation for the dependence of the kinetic constant on the temperature, the apparent activation energy was 39.4 kJ/mol. The half-life for the disappearance of epoxide groups was calculated to be 26 and 10 min at 150 and 200°C, respectively. On the other hand, the kinetic constants for the disappearance of primary amine groups were  $1.58 \times 10^{-4}$ ,  $10.1 \times 10^{-4}$ , and  $18.6 \times 10^{-4} \text{ s}^{-1}$  when curing at 120, 150, and 200°C, respectively. In this case, the apparent activation energy was 37.7 kJ/mol. Therefore, the activation barrier for primary amine groups is quite similar to that obtained for epoxide groups, as previously reported when using first-order kinetics.

As shown in Figure 8, the adjustments of experimental conversion data (for both epoxide and pri-

**TABLE II**  
Kinetic Constant and Activation Energy Values Obtained by Linear Regression (According to Avrami Equation) for the Curing Process of the Nanocomposites

T (°C)	Epoxide groups			Primary amine groups		
	n	k (s <sup>-1</sup> )	r <sup>2</sup>	n	k (s <sup>-1</sup> )	r <sup>2</sup>
120	0.90	$1.25 \times 10^{-4}$	0.985	0.89	$1.58 \times 10^{-4}$	0.959
150	0.93	$7.29 \times 10^{-4}$	0.969	0.80	$10.1 \times 10^{-4}$	0.942
200	1.03	$9.42 \times 10^{-4}$	0.924	0.78	$18.6 \times 10^{-4}$	0.963
			$E_a = 39.4 \text{ kJ/mol}$	$E_a = 37.7 \text{ kJ/mol}$		

mary amine groups) to the selected kinetic models (first-order kinetics and Avrami equation) were, in general, excellent. It was observed a better adjustment by using first-order kinetics in the final stages of curing because of the use of the asymptotic conversion value into the kinetic equation, as previously described. The Avrami equation led to better adjustments in the initial stages of curing.

Figure 9 shows the comparison of curing conversion at 120°C (5% MMT content) by using two different techniques: FTIR spectroscopy (epoxide band at  $906 \text{ cm}^{-1}$ ) and DSC. The results clearly indicated that the progress of curing reactions can be monitored by both techniques, because they provide similar conversion values. This finding validates again the correctness of the FTIR bands used in our study.

## CONCLUSIONS

In the initial stages of the thermal cycle curing, it was observed that a greater proportion of MMT in the nanocomposite led to higher epoxide conversions (as determined by FTIR spectroscopy). After 2 h at 100°C, the epoxide conversions were 11, 25, and 44%

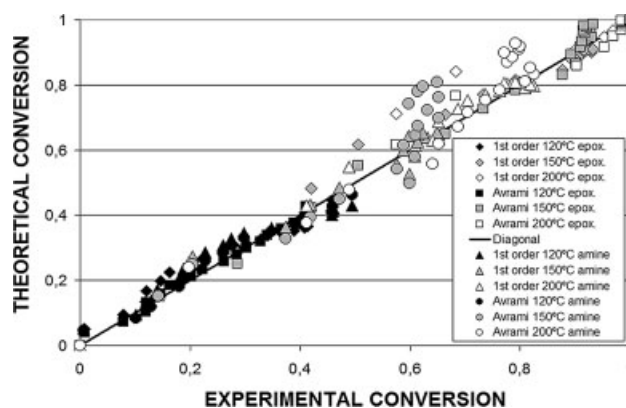


**Figure 8** Comparison of theoretical (first-order kinetics and Avrami equation) and experimental conversion data for both epoxide and primary amine groups.

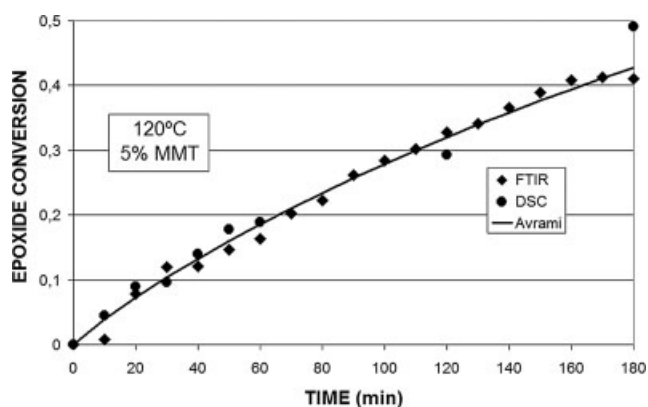


**Figure 9** Comparison of curing conversion at 120°C, by using FTIR spectroscopy (epoxide band at 906  $\text{cm}^{-1}$ ) and DSC.

for 2, 5, and 10% MMT content, respectively, and the mean reaction rates were 5.5, 12.5, and 22%/h. On the contrary, in the final stages of curing, the MMT nanoparticles cancels out, and invert the accelerant effect due to the fact that a higher concentration of particles creates a physical barrier that increasingly hinders completion of the covalent crosslinking between the resin chains. Total curing of the matrix was attained after 4 h at 100°C, 2 h at 150°C, and 1 h of heat treatment at 200°C for all the nanocomposites studied. The absence of the octadecyl ammonium accelerant led to slower curing at all stages and total curing required longer heat treatment of the system.

The epoxide conversion was slightly lower than the amine conversion, within the conversion range 0–70%. It was demonstrated that there is a linear relationship between epoxide and amine conversions ( $\alpha_{\text{epoxide}} \approx 0.93 \alpha_{\text{amine}}$ ). Therefore, reactions (other than addition reactions between epoxide and primary amine groups) must exist that are responsible for the consumption of epoxide groups. At higher conversions (>80%), there was an inversion of this behavior. Therefore, at the end of the nanocomposite curing, the epoxide groups were totally consumed whereas the amine conversion was about 87–92%. This can be explained by taking into consideration that the hardener is present in a slight excess (as confirmed by the presence of an endothermic peak at  $\sim 180^\circ\text{C}$ ).

The isothermal trials were used to determine the best kinetic models. Our experimental data presented poor adjustment when using the autocatalytic kinetic model whereas there was an excellent correlation when the first-order kinetic model and Avrami equation were employed. In the first-order kinetics model, the traditional equations were modified by changing 1 by the asymptotic conversion reached at each temperature:  $\alpha_m$  (epoxide groups) =

0.41, 0.93, and 1 for 120, 150, and 200°C, respectively, and  $\alpha_m$  (primary amine groups) = 0.50, 0.66, and 0.83. The kinetic constants for the disappearance of epoxide and primary amine groups were quite similar when using these two kinetic models because of the  $n$  exponent (in Avrami equation) was found to be very close to 1. The apparent activation energy for the disappearance of epoxide groups, within the temperature range studied, was 29.5 (first-order kinetics) and 39.4 kJ/mol (Avrami equation). These values were very close to those evaluated for the disappearance of primary amine groups: 24.4 and 37.7 kJ/mol. Therefore, the activation barrier for the epoxide groups and primary amine groups was quite similar, thus confirming that the main reaction during the curing process was the polymerization between epoxide and primary amine groups. The activation energy values for the nanocomposites studied were lower than those reported for epoxy resins without nanoparticles (up to 89 kJ/mol), thus indicating the accelerant effect of the MMT nanoparticles in the curing process of epoxy resins. Finally, it was shown that the conversions calculated by FTIR spectroscopy (epoxide band at 906  $\text{cm}^{-1}$ ) and DSC were quite similar.

The authors thank Dr. J. Hutchinson, visiting professor at Universitat Politècnica de Catalunya (UPC), for his valuable contribution in the experimental section and F. J. Barahona (UPC) for his technical assistance. One of the authors (M. L.) thanks the Ministry of Education and Science of the Spanish Government for financing her research stay at the Department of Material Science of the UPC.

## References

- Xu, W.; Bao, S.; He, P. *J Appl Polym Sci* 2002, 84, 842.
- Xu, W.; Bao, S.; Shen, S.; Wang, W.; Hang, G.; He, P. *J Polym Sci Part B: Polym Phys* 2003, 41, 378.
- Xu, W.; Bao, S.; Shen, S.; Hang, G.; He, P. *J Appl Polym Sci* 2003, 88, 2932.
- Zhang, K.; Wang, L.; Wang, F.; Wang, G.; Li, Z. *J Appl Polym Sci* 2003, 91, 2649.
- Becker, O.; Simon, G. P.; Varley, R. J.; Halley, P. *J Polym Eng Sci* 2004, 43, 850.
- Hartwig, A.; Sebald, M.; Pütz, D.; Aberle, L. *Macromol Symp* 2005, 221, 127.
- Jia, Q.; Zheng, M.; Cheng, J.; Chen, H. *Polym Int* 2006, 55, 1259.
- Gârea, S.; Iovu, H.; Stoleriu, S.; Voicu, G. *Polym Int*; 2007, 56, 1106.
- Someya, Y.; Shibata, M. *Polym Eng Sci* 2004, 44, 2041.
- Chong, K. P. *J Phys Chem Solids* 2004, 65, 1501.
- Ray, S. S.; Okamoto, M. *Prog Polym Sci* 2003, 26, 1539.
- Tan, E. P. S.; Lim, C. T. *Compos Sci Technol* 2006, 66, 1101.
- Sánchez-Soto, M.; Pagès, P.; Lacorte, T.; Briceño, K.; Carrasco, F. *Comp Sci Technol* 2007, 67, 1974.



14. Hackman, I.; Hollaway, L. *Appl Sci Manuf* 2006, 37, 1161.
15. Carrasco, F.; Pagès, P.; Lacorte, T.; Briceño, K. *J Appl Polym Sci* 2005, 98, 1524.
16. Mustata, F.; Bicu, F. *J Appl Polym Sci* 2000, 77, 2430.
17. Becker, O.; Cheng, Y. B.; Rusell, J. V.; Simon, G. P. *Macromolecules* 2003, 36, 1616.
18. Kommann, X.; Lindberb, H.; Berglund, L. A. *Polymer* 2001, 42, 4493.
19. Alexandre, M.; Dubois, P. *Mater Sci Eng R Rep* 2000, 28, 1.
20. Chin, I. J.; Albrecht, T. T.; Kim, H. C.; Rusell, T. P.; Wang, J. *Polymer* 2001, 42, 5947.
21. Triantafillidis, C. S.; Le Baron, P. C.; Pinnavaia, T. J. *J Solid State Chem* 2002, 167, 354.
22. Varley, R. J.; Liu, W.; Simon, G. P. *J Appl Polym Sci* 2006, 99, 3288.
23. Ton-That, M. T.; Ngo, T. D.; Ding, P.; Fang, G.; Cole, K. C.; Hoa, V. *Polym Eng Sci* 2004, 44, 1132.